Journal of Neuroimmunology 334 (2019) 576973

Contents lists available at ScienceDirect

Journal of Neuroimmunology

journal homepage: www.elsevier.com/locate/jneuroim

Activation of microglia and macrophages in the circumventricular organs of the mouse brain during TLR2-induced fever and sickness responses

Saki Murayama, Erkin Kurganov, Seiji Miyata*

Department of Applied Biology, Kyoto Institute of Technology, Matsugasaki, Sakyo-ku, Kyoto 606-8585, Japan

ARTICLE INFO

Keywords:
TLR4
LPS
Inflammation
NF-κB
Fos
Brain

ABSTRACT

Toll-like receptor 2 (TLR2) recognizes cell wall components from Gram-positive bacteria. Until now, however, little has been known about the significance of brain TLR2 in controlling inflammation and thermoregulatory responses during systemic Gram-positive bacterial infection. In the present study, the TLR2 immunoreactivity was seen to be prominent in the microglia/macrophages of the circumventricular organs (CVOs) of the mouse brain. The intraperitoneal injection of Pam3CSK4, a TLR2 agonist, induced nuclear factor-κ B activation in the microglia/macrophages of the CVOs. The injection of Pam3CSK4 also produced the expression of Fos at astrocytes and neurons in the CVOs and the regions neighboring the CVOs. The Pam3CSK4 injection induced fever and sickness responses. Pretreatment with lipopolysaccharide, a TLR4 agonist, augmented the Pam3CSK4-induced fever together with the increased TLR2 immunoreactivity. These results indicate that the TLR2 in microglia/macrophages of the CVOs are possibly associated with initiating and transmitting inflammatory responses in the brain.

1. Introduction

Toll-like receptors (TLRs) have been shown to play a critical role in the induction of innate and inflammatory responses when bacteria and viruses invade the bodies of humans and rodents (Akira et al., 2001; Gay et al., 2014). TLRs are a receptor that recognizes pathogen-associated molecular patterns (PAMPs), which play crucial roles in early innate recognition and host inflammatory responses against invading disease-causing microbes (Akira et al., 2001). Among the TLR family members, TLR2 recognizes a variety of TLR2 ligands from all microbial phyla, including viruses, fungi, bacteria, and parasites (Zahringer et al., 2008; Oliveira-Nascimento et al., 2012). This diversity depends on TLR2 having a vast array of ligands, including lipoproteins, lipoteichoic acid, proteins, polysaccharides, and peptidoglycans (Schwandner et al., 1999; Oliveira-Nascimento et al., 2012), and TLR2 having the ability to form functional heterodimers with two other types of TLRs and a large number of non-TLR molecules (Zahringer et al., 2008; Oliveira-Nascimento et al., 2012). The most well-characterized TLR2 ligands thus far are lipoproteins, which are ubiquitous to all bacteria and which are highly expressed in the outer membrane of Gram-positive bacteria (Nguyen and Gotz, 2016), while triacyl and diacyl lipoproteins are recognized by TLR2/TLR1 and TLR2/TLR6, respectively (Beutler et al., 2006; Botos et al., 2011).

TLR2 heterodimers generally initiate a MyD88-dependent intracellular signaling pathway so that nuclear factor-κ B (NF-κB) translocates into the nucleus to modulate gene transcription and consequent inflammatory cytokine production (Kawai and Akira, 2010). The cascade also activates serine/threonine-specific protein kinases, which influence both the transcription and mRNA stability of inflammatory genes (Kawai and Akira, 2010). The systemic injection of TLR2/6 agonist results in fever and increases the tumor necrosis factor-α (TNF-α) and interleukin-6 (IL-6) levels in the plasma, but these responses are entirely blunted in TLR2-knockout (KO) mice (Welsch et al., 2012).

The blood-brain barrier (BBB) is a highly specialized brain endothelial structure that separates the circulating blood from the brain to maintain a constant homeostatic environment in the brain parenchyma (Zlokovic, 2011). The circumventricular organs (CVOs) are characterized by highly permeable fenestrated capillaries unlike those in the rest of the brain (Morita and Miyata, 2012; Morita et al., 2016). These consist of the organum vasculosum of the lamina terminalis (OVLT), subfornical organ (SFO), median eminence (ME) and area postrema (AP) (Sisó et al., 2010; Miyata, 2015). The CVOs function as the blood-brain interface for communicating between the brain parenchyma cells and peripheral organs *via* blood circulation to initiate the earlier inflammatory response (Roth et al., 2004; Sisó et al., 2010; Miyata, 2015). Our previous studies revealed that the TLR4 or

* Corresponding author at: Department of Applied Biology, Kyoto Institute of Technology, Kyoto 606-8585, Japan.
E-mail address: smiyata@kit.ac.jp (S. Miyata).

https://doi.org/10.1016/j.jneuroim.2019.576973
Received 27 April 2019; Received in revised form 26 May 2019; Accepted 27 May 2019

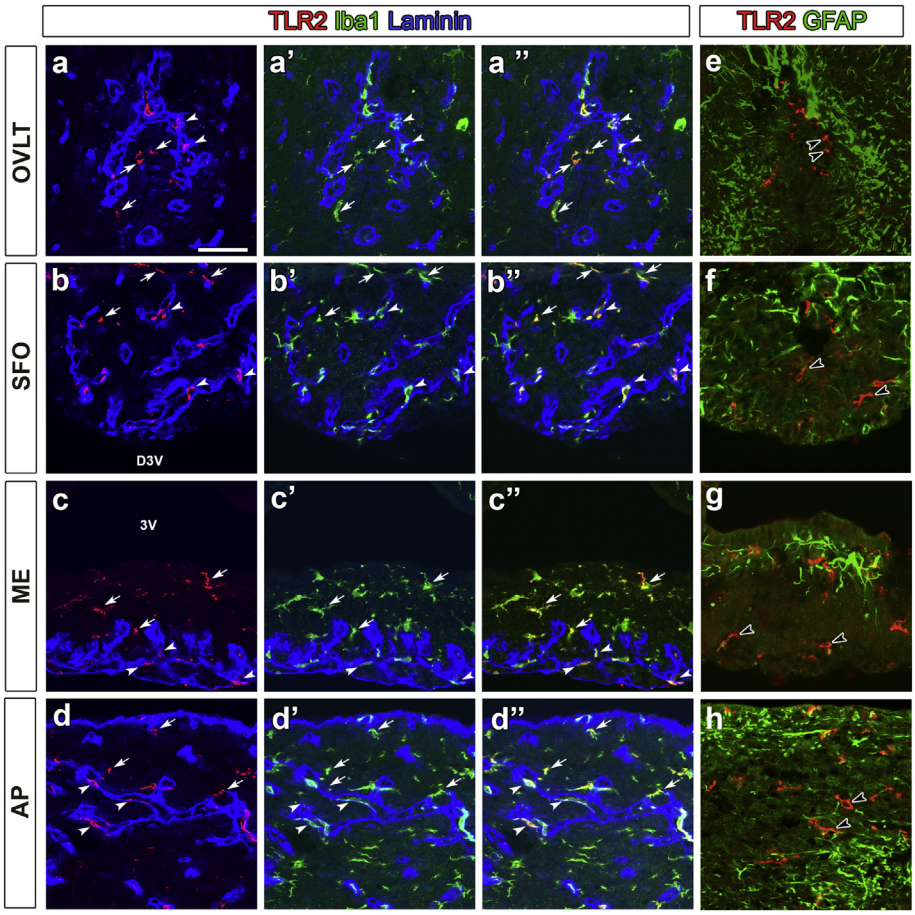

Fig. 1. The expression of TLR2 of the microglia/macrophages in the CVOs of the mouse brain under basal/unstimulated conditions. a–d, a′–d′, a″–d″: Triple-labeling immunohistochemistry images showing the TLR2 immunoreactivity of the Iba1$^+$ microglia (open arrows) and macrophages (arrowheads) and laminin$^+$ perivascular space in the CVOs. Microglia were localized at parenchyma or outside the capillary, whereas macrophages were present in the perivascular space. e-h: Double-labeling immunohistochemistry revealed that visible TLR2 immunoreactivity (solid arrows) was not observed in the GFAP$^+$ astrocytes in the CVOs. Scale bars = 50 μm. 3 V, 3rd ventricle; D3V, dorsal 3rd ventricle.

lipopolysaccharide (LPS) receptor was highly expressed in the CVOs of the mouse brain NF-κB (Quan et al., 1997; Chakravarty and Herkenham, 2005; Muneoka et al., 2019). Astrocytes in the CVOs are known to have neural stem cell-like properties (Furube et al., 2015). In comparison to other regions of the brain, circulating LPS/cytokines cause the faster transcriptional activation of genes encoding a wide variety of proinflammatory molecules in the CVOs; including nuclear factor-κ B (NF-κB; Quan et al., 1997; Chakravarty and Herkenham, 2005; Muneoka et al., 2019) and the signal transducer and activator of transcription factor 3 (STAT3; Rummel et al., 2004, 2005; Nakano et al., 2015; Yoshida et al., 2016). The systemic injection of LPS preferentially increases the tumor necrosis factor (TNF)-α, interleukin (IL)-1β, and IL-6 levels in the CVOs (Breder et al., 1994; Vallieres and Rivest, 1997; Chakravarty and Herkenham, 2005). The TLR4 in the astrocytes and tanycytes of the CVOs has also been shown to act as a central regulator for preventing the overshoot of fever during LPS-induced inflammatory conditions and for maintaining a proper body temperature during normal conditions (Muneoka et al., 2019). Thus, evidence is accumulating to support that the TLR4 in the CVOs has a crucial function in initiating and controlling the inflammatory responses after systemic LPS stimulation.

Gram-positive bacteria are common causes of nosocomial bloodstream infection, and the prevalence of infections caused by antibiotic-resistant gram-positive bacteria is increasing (Rice, 2006). The activation of TLR2 in immune cells by lipoproteins is a significant factor in Gram-positive sepsis (Takeuchi et al., 2000; Hashimoto et al., 2006). The systemic injection of macrophage-activating lipopeptide-2 of *Mycoplasma fermentans* induces the activation of STAT3 in a subpopulation of parenchyma cells in the CVOs (Knorr et al., 2008). The intracerebroventricular (i.c.v.) injection of Pam3CSK4, a TLR2 ligand, has been shown to lead to sickness responses, including anorexia, hypoactivity, and fever through the hypothalamic arcuate nucleus (Jin et al., 2016). A robust and temporal elevation of the TLR2 mRNA expression occurs in the CVOs after the systemic injection of LPS, although the injection of lipoteichoic acid peptidoglycans, a TLR2 agonist, or the combination of both substances does not alter the TLR2 mRNA expression (Laflamme and Rivest, 2001; Rivest, 2003, 2009), indicating the occurrence of crosstalk between TLR4 and TLR2. The involvement of the TLR2 in the brain in inflammatory signaling and responses appears to have little functional significance, despite the importance of TLR2 in various infection processes.

In the present study, we therefore aimed to investigate the TLR2-dependent activation of microglia/macrophages and following glial-neuronal circuits to control the inflammatory response in the adult mouse brain. First, the stronger TLR2 immunoreactivity was observed in the microglia/macrophages of the CVOs in comparison to other brain regions under basal/unstimulated conditions. Second, the intraperitoneal injection of Pam3CSK4, a TLR2 ligand, caused the activation of NF-κB in the microglia/macrophages of the CVOs. Third, Pam3CSK4 induced the expression of Fos in the astrocytes of the CVOs and neurons in the inflammation-regulating brain regions. Finally, the pretreatment with LPS, a TLR4 agonist, significantly increased the expression levels of TLR2 in the CVOs and augmented the Pam3CSK4-induced fever. Thus, the present study indicates that the TLR2 in the microglia/macrophages of the CVOs probably plays a role in initiating and controlling fever and the sickness responses induced by Gram-positive bacteria.

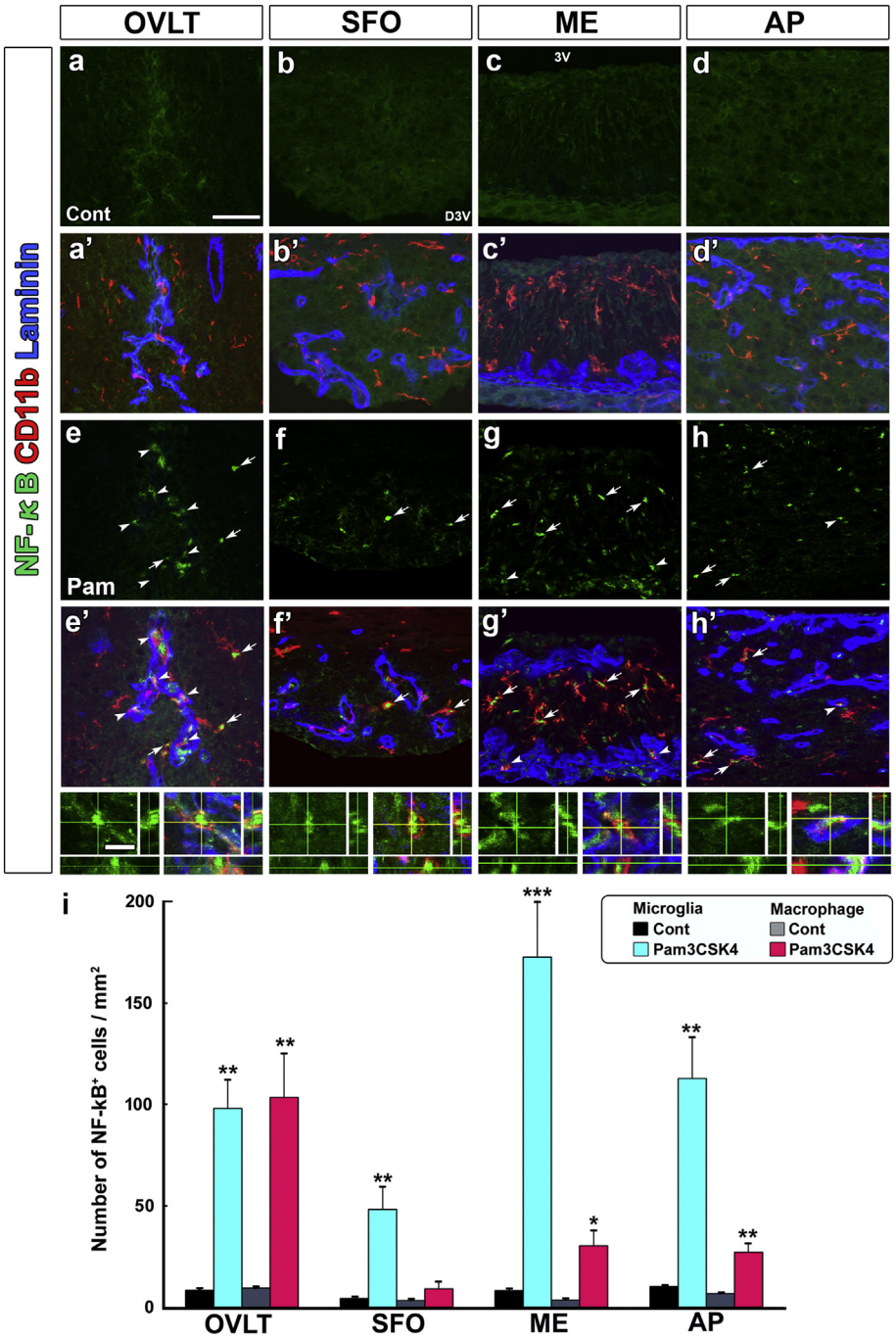

Fig. 2. Activation of NF-κB in the microglia/macrophages in the CVOs of mice following the single systemic injection of Pam3CSK4, a TLR2 agonist. Mice received an intraperitoneal injection of Pam3CSK4 (1 mg/kg) and were sacrificed for NF-κB immunohistochemistry 2 h after the injection. a–d, a′–d′: NF-κB nuclear translocation was rarely observed in control mice. e–h, e′–h′: The nuclear translocation of NF-κB was seen in both the Iba1$^+$ microglia (arrows) and macrophages (arrowheads) of Pam3CSK4-injected mice (upper panels in e′–h′). A three-dimensional image analysis demonstrated the presence of NF-κB-immunoreactive nuclei in CD11b$^+$ microglia and macrophages (lower panels in e′–h′). Scale bars = 50 (a), 10 (bottom in e′) μm. i: A quantitative analysis showed that the number of NF-κB$^+$ microglia/macrophages was significantly increased after the Pam3CSK4 injection. Data (n = 4) are expressed as the mean (± s.e.m.). *: $P < 0.05$, **: $P < 0.01$, ***: $P < 0.001$ between the control and Pam3CSK4 mice (unpaired Student's t-test).

2. Material and methods

2.1. Animals

Male ICR mice (70–105 days old; Japan SLC Inc., Hamamatsu, Japan) were housed in a colony room (24 ± 0.5 °C) with a 12-h light/dark cycle; light on at 7:00 and light off at 19:00 and given *ad libitum* access to commercial chow and tap water. All experiments were performed according to the guidelines laid down by the NIH and Proper Conduct of Animal Experiments Science Council of Japan. An antibiotic, enrofloxacin (Baytril, Bayer Yakuhin Ltd., Tokyo, Japan), was added to the drinking water (170 mg/l) of the mice for several days after surgery to protect them from infection. The protocols of all experiments were approved by the animal care and use committee of the Kyoto Institute of Technology.

2.2. Injection of drugs

Pam3CSK4 (MW 1510.2) and synthetic triacylated lipopeptide were purchased from Tocris Bioscience (Catalog No. 4633, Bristol, UK) and Merck (M9511, Sigma-Aldrich Japan, Tokyo, Japan), respectively. The Pam3CSK4 was dissolved in distilled deionized pathogen-free water at the concentration of 0.8 mg/ml and stored at −80 °C until use. For the immunohistochemistry of NF-κB and Fos, animals were sacrificed 2 h after single intraperitoneal injection of 1 mg/kg Pam3CSK4 (200 μl, 0.8 mg/ml) or distilled deionized water (DDW). For LPS pretreatment, mice received a single intraperitoneal injection (100 μl) of LPS (100 μg/kg; Sigma-Aldrich, 055: type B5) 24 h before a single intraperitoneal injection of Pam3CSK4 (1 mg/kg; 0.8 mg/ml) or DDW. The dose (100 μg/kg) of LPS is shown to induce fever and sickness responses in our previous studies (Furube et al., 2018; Muneoka et al., 2019). The

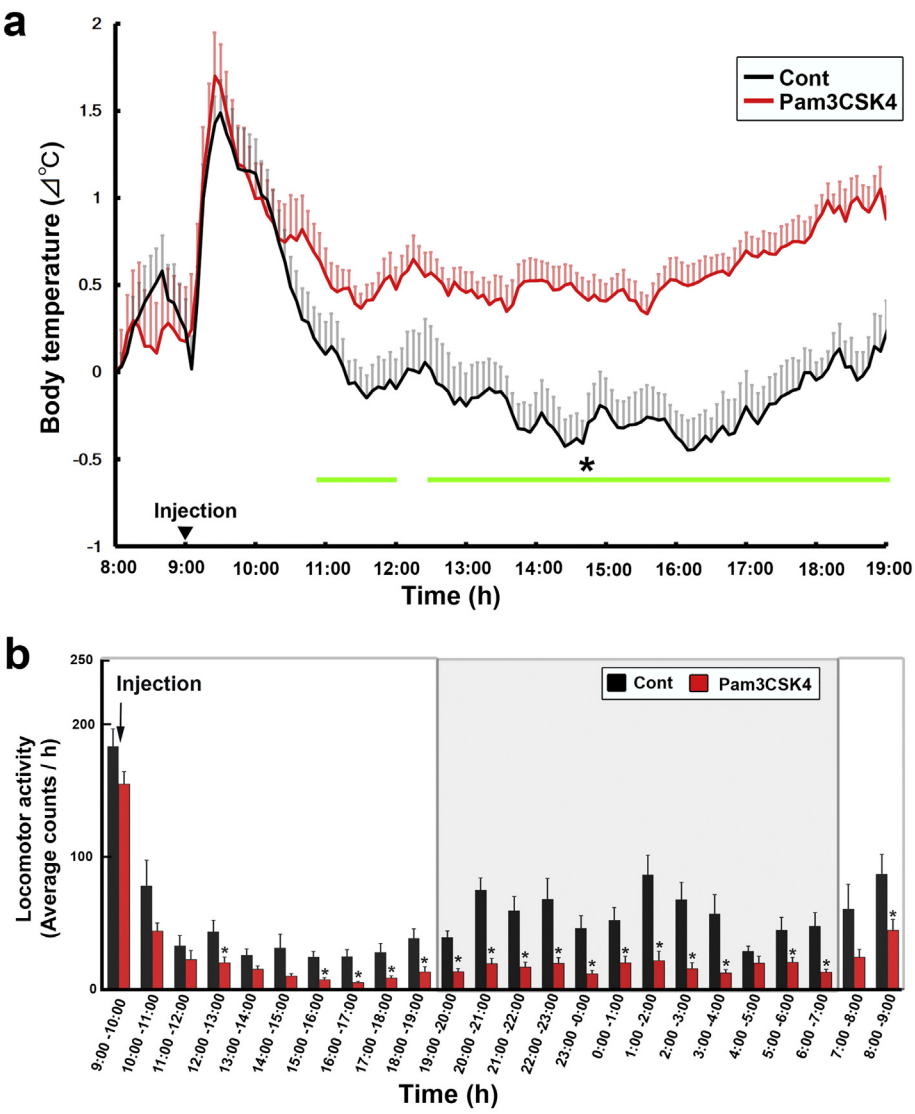

Fig. 3. The systemic injection of Pam3CSK4 (a TLR2 agonist) induces fever and reduces the locomotor activity of mice. The abdominal core temperature and locomotor activity were measured by the G2 *E*-mitter telemetry system after the intraperitoneal injection of Pam3CSK4 (1 mg/kg) in the ambient temperature at 24 ± 0.5 °C. Mice of both control and Pam3CSK4-stimulated groups initially showed stress-induced fever during/after the injection procedure. a: The intraperitoneal injection of Pam3CSK4 induced marked continuous fever. Mice initially exhibited a stress-induced increase in body temperature during/after the injection procedure. The green line indicates the period in which the body temperature differed between the control and Pam3CSK4-injected mice. b: Pam3CSK4-injected mice showed decreased locomotor activity in comparison to control mice. Data (n = 10) are expressed as the mean (± s.e.m.). *: $P < 0.05$ between the control and Pam3CSK4 mice (unpaired Student's t-test). (For interpretation of the references to colour in this figure legend, the reader is referred to the web version of this article.)

dose (1 mg/kg) of Pam3CSK4 is shown to evoke a cytokine response similar to 1 mg/kg of LPS (Mersmann et al., 2010).

2.3. Immunohistochemistry

After deep anesthesia with isoflurane, mice were intracardially perfused with phosphate-buffered saline (PBS; pH 7.4) containing 0.1% trisodium citrate dihydrate by 4% paraformaldehyde in 0.1 M phosphate buffer (PB; pH 7.4). Fixed brains were cryoprotected by 30% sucrose in PBS (pH 7.4) and frozen quickly in Tissue-Tek OCT compound (Sakura Finetechnical, Tokyo, Japan). Sections were obtained by a coronal cut on a cryostat (Leica, Wetzlar, Germany) at a thickness of 30 µm. For immunofluorescence labeling, a standard technique applied to free-floating sections, as described in our previous study (Furube et al., 2018). In brief, the sections were washed with PBS and treated with 25 mM glycine in PBS for 20 min to quench the remaining aldehyde moiety. Sections were preincubated with 5% normal goat serum (NGS) in PBS containing 0.3% Triton X-100 (PBST) at 4 °C for 24 h and then incubated with the primary antibody in PBST containing 1% NGS at 4 °C for 72 h. The following primary antibodies were used: mouse monoclonal antibody against HuC/D (clone 16A11, Molecular Probes, ThermoFischer Scientific Japan; dilution 1:400); goat polyclonal antibody against SOX2 (sc-17,320, Santa Cruz Biotechnology, Sant Cruz, CA; dilution 1:2000 or Cat. No. AF 2018, R&D Systems, Minneapolis, MN; dilution 1:2000); rabbit polyclonal antibody against Fos (Cat. No. sc-52, Santa Cruz Biotechnology; dilution 1:3000), NF-κB p65 (Cat. No. sc-372, Santa Cruz Biotechnology; dilution 1:1000), and Iba1 (Cat. No. 019–19,741, FUJIFILM Wako Chemicals, Tokyo, Japan; dilution 1:800); rat monoclonal antibody against TLR2 (clone T2.5, eBioscience, ThermoFischer Scientific Japan, Tokyo, Japan, dilution 1:1000) and CD11b (clone 5C6, BioRad, ThermoFischer Scientific Japan; dilution 1:10,000); and guinea pig polyclonal antibody against glial fibrillary acidic protein (GFAP; H29–1127; dilution 1:400, Muneoka et al., 2019) and laminin (the antigen was laminin-111 from Engellbreth-Holm-Swarm murine sarcoma basement membrane: IM-2011; dilution 1:200, Imamura et al., 2010). After several washes with PBST, they were further incubated with an Alexa 405-, 488- or 594-conjugated secondary goat antibody (Jackson ImmunoResearch, West Grove, PA, dilution 1:400). When the mouse primary antibody was used, Alexa 594-conjugated goat F(ab)$_2$ against mouse IgG (Jackson ImmunoResearch; dilution 1:100) was used to avoid the binding of endogenous Fc receptors. For the confocal microscopic observations, coverslips were sealed with Vectashield (Vector Labs, Burlingame, CA) and observations were performed using a laser-scanning confocal microscope (Olympus FV 10i, Tokyo, Japan).

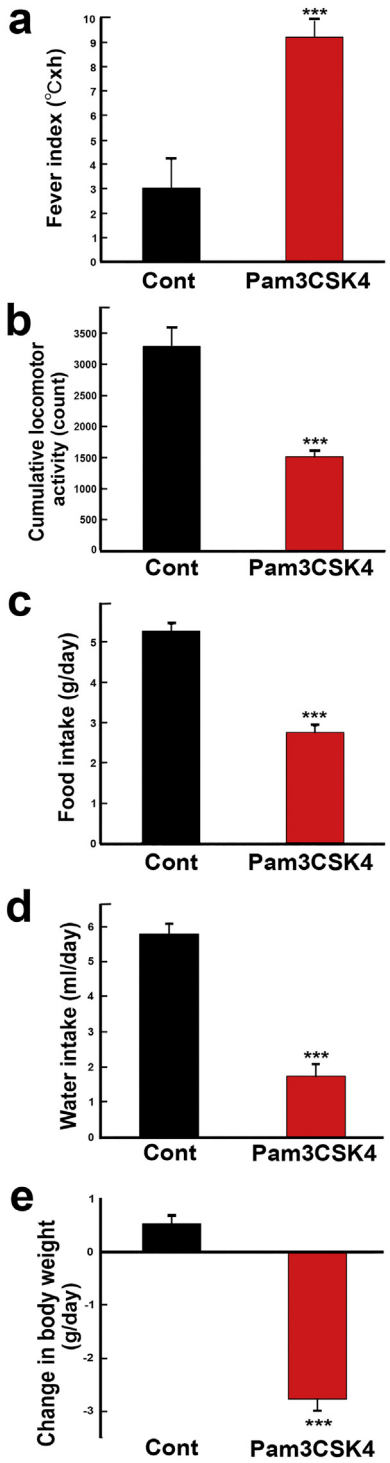

Fig. 4. The systemic injection of Pam3CSK4 causes sickness responses in mice. Mice received an intraperitoneal injection of Pam3CSK4 (1 mg/kg) and vehicle or DDW (control). The fever index and cumulative locomotor activity were calculated during daytime (10:30–19:00), and the food and water intake and change in body weight were measured for 24 h after the injection. a: The fever index of Pam3CSK4-injected mice was significantly higher in comparison to the control mice. b-d: The cumulative locomotor (b), food (c) and water intake (d) and change in body weight (e) were significantly reduced in Pam3CSK4-treated mice. Data (n = 10) are expressed as the mean (± s.e.m.). ***: $P < 0.001$ between the control and Pam3CSK4 mice (unpaired Student's *t*-test).

2.4. Measurement of body temperature

The measurement of body temperature and locomotor activity was performed according to the methods of our previous studies (Yoshida et al., 2016; Muneoka et al., 2019). Mice were anesthetized with isoflurane and underwent the implantation of a G2 *E*-mitter telemetry system implant (Star Life Science Co., Oakmont, PA) *via* a midline laparotomy. The implanted system, which was sutured to the dorsolateral abdominal wall, was kept for at least one week. Mice received an intraperitoneal injection of Pam3CSK4 (200 µl, 1 mg/kg) or DDW between 09.00 and 09.30. The measurement of the abdominal temperature and locomotor activity was performed using the G2 E-mitter telemetry system implant at 5-min intervals and plotted at 10-min intervals from 12 h before to 12 h after the injection of Pam3CSK4 or distilled deionized water. Mice received an intraperitoneal injection (200 µl) of Pam3CSK4 (1 mg/kg) or distilled deionized water on the fourth day. For LPS pretreatment, the animals received an intraperitoneal injection of LPS (100 µg/kg) 24 h before Pam3CSK4 stimulation. Data were acquired and fed to a computer using the Vital View software program (Vital View series 4000, Star Life Science Co). The fever index (°C x h) was calculated as the area under the temperature curve based on the mean temperature during a period of 2 h before the intraperitoneal injection.

2.5. Confocal and statistical analysis

For quantitative analysis, we selected at least five sections per animal from the OVLT and seven sections per animal from the other brain regions according to the mouse brain atlas (Paxinos and Franklin, 2001). Confocal images were obtained under the same pinhole size, brightness, and contrast settings. We saved images (1024 × 1024 pixels) as TIF files using the Olympus Fluoview Ver. 4.2a viewer and arranged them using the Photoshop CC software program (Adobe Creative Cloud, San Jose, CA). In the case of NF-κB and Fos, we set the threshold of contrast setting of the confocal microscope to detect the preferentially strong signal in the nucleus. The numbers of Fos- and NF-κB$^+$ nuclei in the Iba-1-labeled microglia/macrophages, SOX2-labeled astrocytes, and HuC/D-labeled neurons were counted using WinRoof, an image analysis system (Mitani Corporation, Fukui, Japan). The relative TLR2 immunoreactivity was calculated by obtaining the percentage of TLR2-immunoreactive area in Iba1$^+$ microglial and macrophagal one. The areas of TLR2-immunoreactive microglia/macrophages and Iba-1-immunoreactive microglia/macrophages were measured using WinRoof (Mitani Corporation). In all of the image analyses, the threshold intensity of which was set to include measurement profiles by visual inspections and was kept constant and the experimenter was blinded to the treatments of the mice.

3. Results

3.1. High expression of TLR2 in the microglia and macrophages of the CVOs

To examine the localization of TLR2-immunoreactive cells in the brain, we performed triple-labeling immunohistochemistry to detect TLR2, Iba1 (microglial/macrophagal marker), and a laminin (a vascular basement membrane marker) in unstimulated mice. Microglia are distinguished from macrophages by their localization since microglia are present on the parenchyma, outside the capillaries, while macrophages are localized in the perivascular space surrounded by a laminin$^+$ basement membrane. TLR2-immunoreactive cells were seen in the OVLT (Fig. 1a), SFO (Fig. 1b), ME (Fig. 1c) and AP (Fig. 1d). Double (Fig. 1a′–d′) and triple (Fig. 1a″–d″) labeling clearly showed the high expression of TLR2 on Iba-1$^+$ perivascular macrophages and parenchyma microglia in the CVOs. On the other hand, double-labeling immunohistochemistry with GFAP (an astrocyte marker) showed that there was no expression of TLR2 on the GFAP$^+$ astrocytes in the OVLT

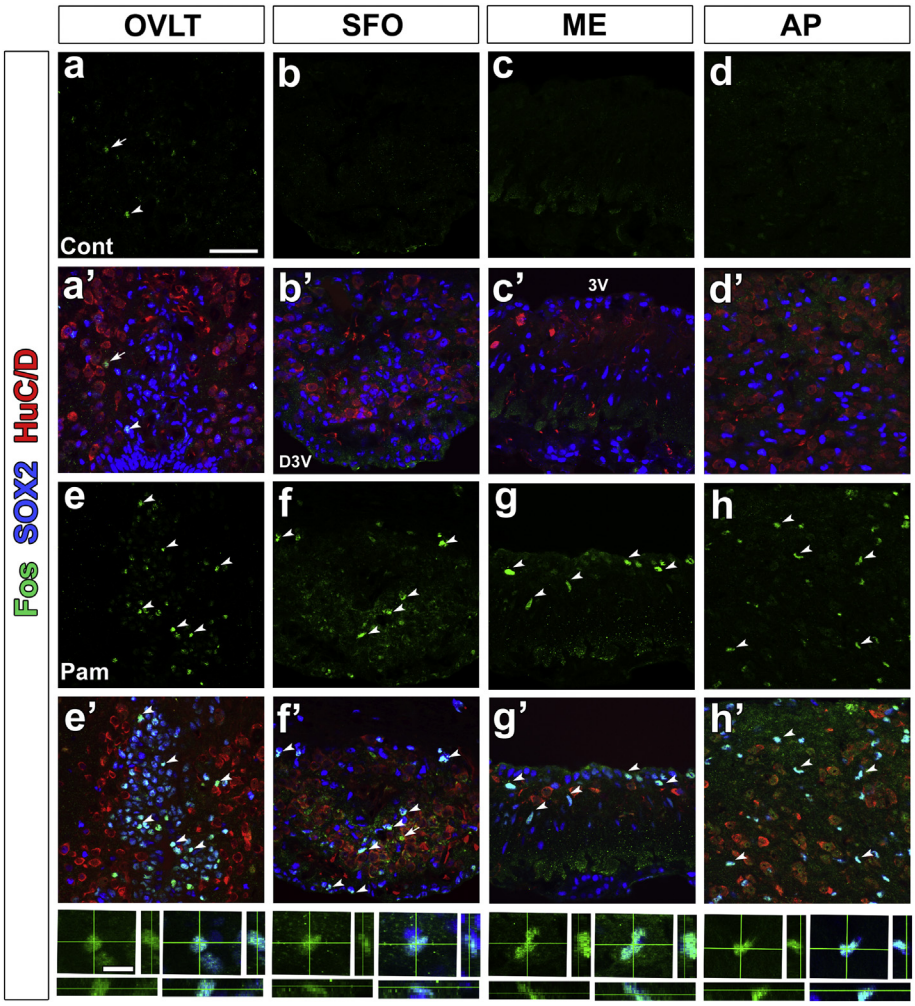

Fig. 5. The effect of the systemic injection of Pam3CSK4 on the Fos expression in the mouse CVOs. Mice received an intraperitoneal injection of Pam3CSK4 (1 mg/kg) or control vehicle. At 2 h after the injection they were sacrificed for Fos immunohistochemistry. a–d, e–h: Representative images showing that the Fos$^+$ cells in the CVOs of Pam3CSK4-treated mice (e–h) were increased in comparison to the control mice (a-d). a′–d′, e′–h′: Triple-labeling immunohistochemistry revealed that Fos$^+$ nuclei were often seen in the SOX2$^+$ astrocytes, but not in the HuC/D$^+$ neurons of Pam3CSK4-injected mice (upper panels in e′–h′), while almost no colocalization was observed in the control mice (a′–d′). A three-dimensional image analysis demonstrated the presence of NF-κB-immunoreactive nuclei in CD11b + microglia and macrophages (lower panels in e′–h′). Scale bars = 50 (a), 10 (bottom in e′) μm. 3 V, 3rd ventricle; D3V, dorsal 3rd ventricle.

(Fig. 1e), SFO (Fig. 1f), ME (Fig. 1g) or AP (Fig. 1h) of the CVOs. GFAP is distributed uniformly over cytoplasm of astrocytes and therefore convenient to visualize the whole astrocytic morphology. These results indicate that TLR2 is highly expressed on the microglia/macrophages of the CVOs in the adult mouse brain.

3.2. Systemic Pam3CSK4 stimulation induces NF-κB activation of the microglia/macrophages in the CVOs

Our previous studies have shown that the nuclear translocation of NF-κB is useful for evaluating NF-κB activation in the brain (Muneoka et al., 2019). We first examined NF-κB activation using an antibody against the NF-κB p65 subunit by immunohistochemistry. There was almost no NF-κB nuclear accumulation or activation in control mice (Fig. 2a–d, a′–d′), while the intraperitoneal injection of Pam3CSK4 (a TLR2 agonist) caused the strong activation of NF-κB in the OVLT (Fig. 2e), SFO (Fig. 2f), ME (Fig. 2g) and AP (Fig. 2h) of the CVOs at a dose of 1 mg/kg. Triple-labeling immunohistochemistry with a microglial marker CD11b and laminin revealed that the NF-κB$^+$ nuclei were present in CD11b$^+$ microglia/macrophages in the CVOs after Pam3CSK4 stimulation (Fig. 2e′–h′), which was confirmed by 3D confocal images (Fig. 2a′–d′). A quantitative analysis revealed an increased number of NF-κB$^+$ cells in the microglia/macrophages of the OVLT (microglia 98.2 ± 14.1; macrophages 103.6 ± 21.4), SFO (microglia 48.3 ± 11.0), ME (microglia 172.7 ± 27.5; macrophages 30.4 ± 7.7) and AP (microglia 112.9 ± 20.3; macrophages 27.2 ± 4.5) of the CVOs after the systemic injection of Pam3CSK4 (Fig. 2i). Thus, these results indicate that NF-κB activation was induced in the microglia/macrophages of the CVO by the systemic injection of Pam3CSK4.

3.3. The Pam3CSK4-induced fever and sickness responses

Since the systemic injection of Pam3CSK4 induces inflammation that mimics Gram-positive bacterial infection, we examined whether or not the systemic injection of Pam3CSK4 changes the body temperature and induces sickness responses. Mice were allowed to move freely and had *ad libitum* access to food and water during the measurement of their body temperature and locomotive activity (Fig. 3). Initially, the mice showed stress-induced fever after the injection of both Pam3CSK4 and DDW, or control vehicle (Fig. 3a). Pam3CSK4-injected mice showed significant fever two hours after the injection. From 3 h after the injection, the locomotive activity of the Pam3CSK4-injected mice was significantly lower than that of the control mice (Fig. 3b).

To understand the Pam3CSK4-induced sickness responses, we showed the cumulative values of fever, locomotor activity, and other factors (Fig. 4). The Pam3CSK4-injected mice showed a 3-fold increase in fever index (9.2 ± 0.7) in comparison to control animals (3.0 ± 1.1) (Fig. 4a). The cumulative locomotor activity decreased from 509.13 ± 42.8 in the control mice to 298.92 ± 12.5 in the Pam3CSK4-injected mice (Fig. 4b). The systemic injection of Pam3CSK4 also significantly reduced the food (Fig. 4c) and water (Fig. 4d) intake from 5.32 ± 0.2 to 2.78 ± 0.2 g and from 5.92 ± 0.3 to 1.78 ± 0.3 ml, respectively. The body weight of Pam3CSK4-injected mice (−0.54 ± 0.2 g) was also significantly lower in comparison to the control mice (+2.77 ± 0.2 g). Taken together, these results

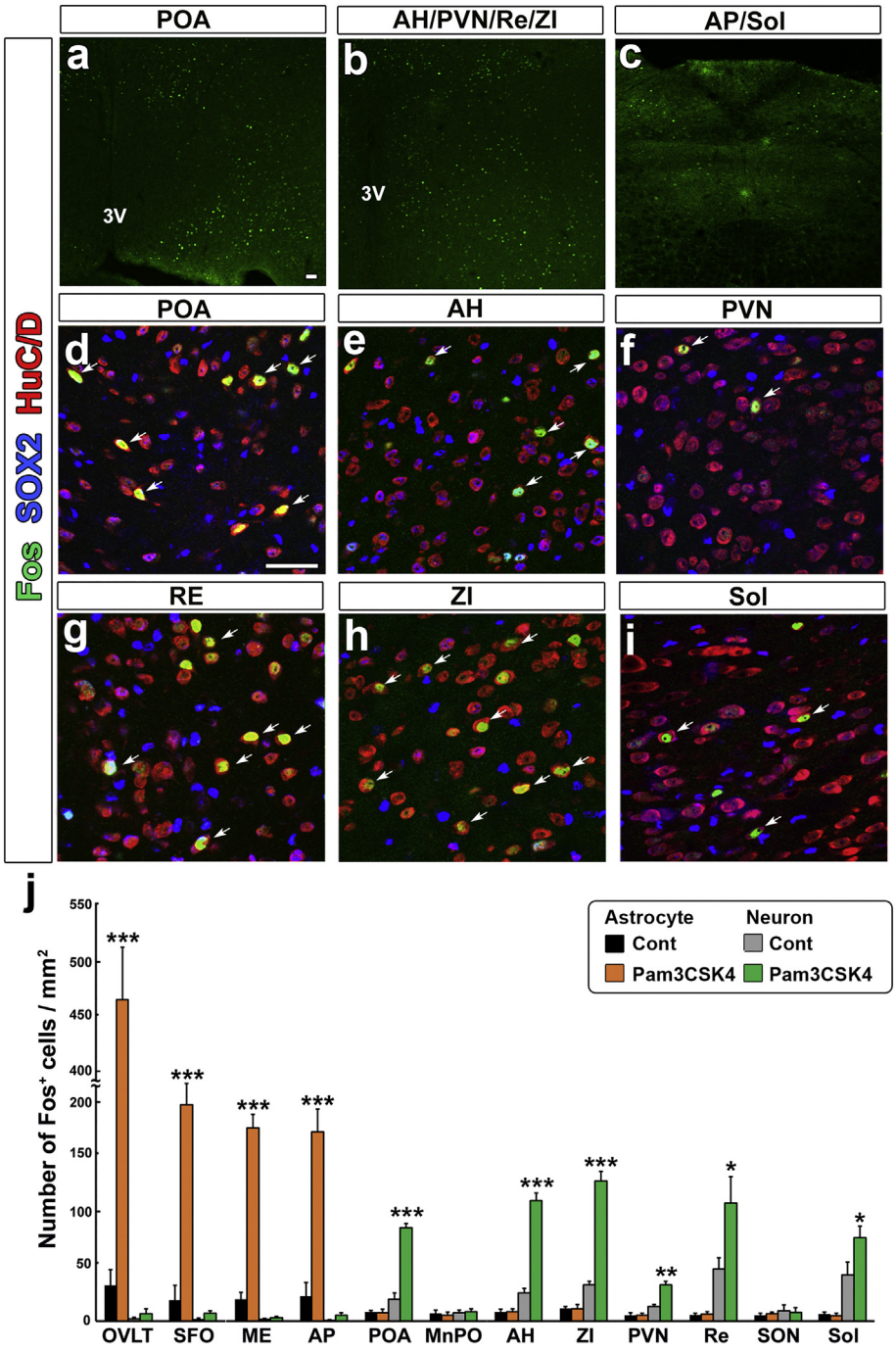

Fig. 6. The effect of the systemic injection of Pam3CSK4 on the Fos expression in the neighboring brain regions and the quantitative analysis of the Fos$^+$ cell density in the mouse brain. Mice received an intraperitoneal injection of Pam3CSK4 (1 mg/kg) or control vehicle. At 2 h after the injection they were sacrificed for Fos immunohistochemistry. a–c: Representative images showing that Fos$^+$ nuclei were observed in the POA, AH, PVN, Re, ZI and Sol of Pam3CSK4-treated mice. d-i: Triple-labeling immunohistochemistry revealed Fos$^+$ nuclei in the HuC/D$^+$ neurons rather than the SOX2$^+$ astrocytes in the Pam3CSK4-treated mice. Scale bars = 50 µm. 3 V, 3rd ventricle. j: The quantitative analysis showed that the number of Fos$^+$ astrocytes was significantly increased in the CVOs, while the number of Fos$^+$ neurons was significantly elevated in the neighboring brain regions. Data ($n = 4$) are expressed as the mean (± s.e.m.). *: $P < 0.05$, **: $P < 0.01$, ***: $P < 0.001$ between the control and Pam3CSK4 mice (unpaired Student's *t*-test).

indicate that systemic injection of the TLR2 agonist Pam3CSK4 causes fever and sickness responses.

3.4. Systemic Pam3CSK4 stimulation induces the expression of Fos in the CVOs and the neighboring brain regions

To examine the brain regions that are activated by the systemic injection of Pam3CSK4, we employed Fos immunohistochemistry to detect activated cells in the brain (Figs. 5 and 6). Control mice showed small numbers of Fos$^+$ cells in the sex determining region Y-box 2 (Sox2)$^+$ astrocytes and HuC/D$^+$ neurons in the OVLT (Fig. 5a, a′), SFO (Fig. 5b, b′), ME (Fig. 5c, c′) and AP (Fig. 5d, d′). SOX2 is localized in the nucleus of astrocytes and therefore convenient to examine Fos$^+$ nucleus in astrocytes. Many Fos$^+$ cells were observed in the CVOs (Fig. 5e–h) after the injection of Pam3CSK4. They were often colocalized with Sox2$^+$ astrocytes, which was confirmed by 3D confocal images, but not with HuC/D neurons (Fig. 5e′–h′). Unlike the CVOs, Fos$^+$ nuclei were more frequently seen in the HuC/D$^+$ neurons of the preoptic area (POA) (Fig. 6a, d), anterior hypothalamic area (AH), paraventricular nucleus (PVN), reuniens thalamic nucleus (Re), zona incerta (ZI) (Fig. 6b, e, f, g, h) and AP/Sol (Fig. 6c, i) in comparison to the control mice (Fig. S1). Using these data, the numbers of Fos$^+$ cells in the CVOs and inflammation-associated brain regions of the adult mouse brain were quantified (Fig. 6j). The systemic injection of Pam3CSK4 significantly increased the numbers of Fos$^+$ astrocytes in the OVLT (465.7 ± 47.8 cells/mm^2), SFO (197.3 ± 19.4), ME (176.2 ± 12.5) and AP (172.6 ± 20.7), whereas the numbers of Fos$^+$ nuclei were only significantly higher in the neurons of the POA, AH, ZI, PVN, Re and Sol (Fig. 6i). These findings indicate that the Pam3CSK-induced expression of Fos is increased in the astrocytes of the CVOs and

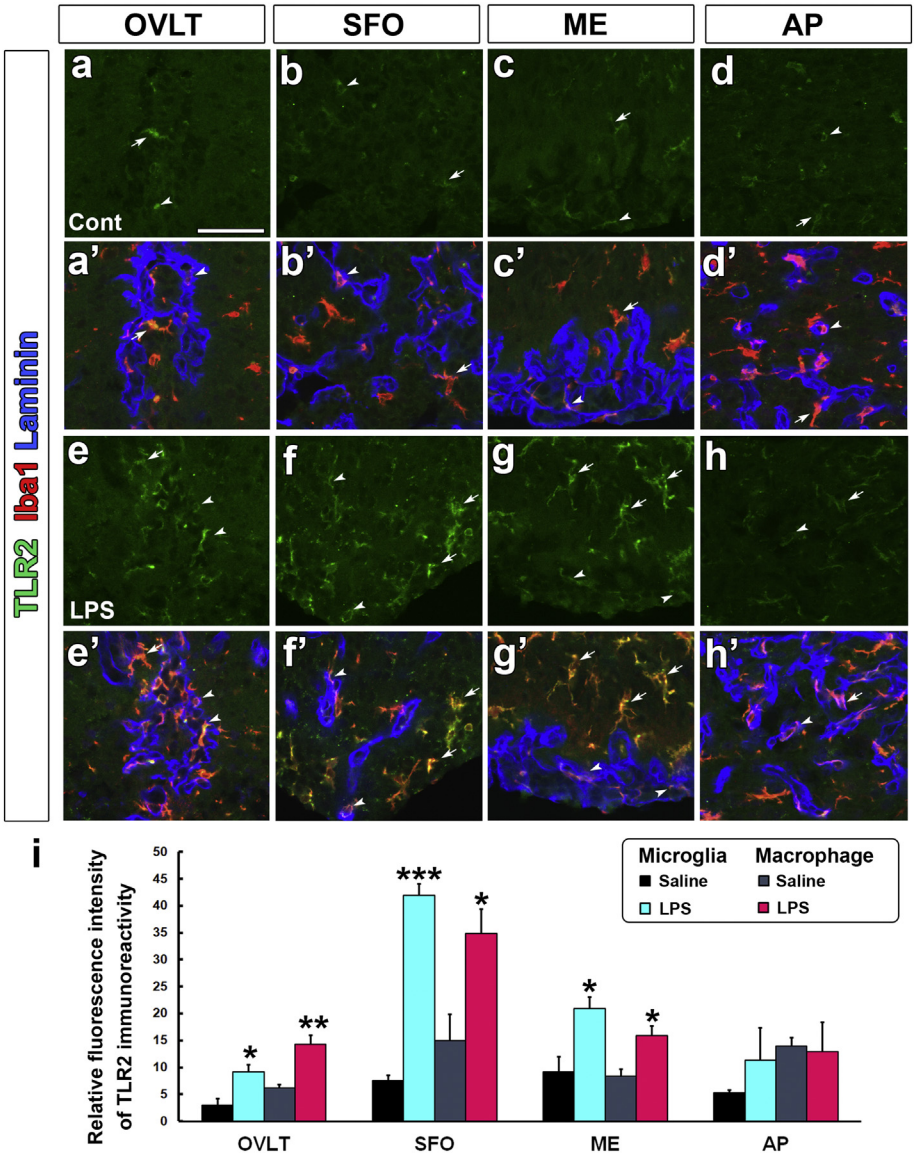

Fig. 7. The systemic injection of LPS increases the TLR2 immunoreactivity of the microglia/macrophages of the CVOs. Mice received an intraperitoneal injection LPS (100 μg/kg) or vehicle saline. At 24 h after the injection they were sacrificed for immunohistochemistry. a–h, a′–h′: The confocal setting of Alexa488 was adjusted so that the fluorescence intensity of TLR2 immunoreactivity was low in the CVOs of the control mice (a–d, a′–d′). In LPS-treated mice, the fluorescence intensity of the TLR2 immunoreactivity was high, even under an identical confocal setting (e–h, e′–h′). Scale bar = 50 μm. i: A quantitative analysis revealed that the fluorescence intensity of TLR2 immunoreactivity was significantly increased by LPS treatment in the microglia/macrophages in the CVOs. Data (n = 4) are expressed as the mean (± s.e.m.). *: $P < 0.05$, **: $P < 0.01$, ***: $P < 0.001$ between the control and Pam3CSK4 mice (unpaired Student's *t*-test).

in the neurons of the brain regions involved in inflammation.

3.5. LPS pretreatment augmented the TLR2-dependent fever and sickness responses

A robust and temporal elevation of the TLR2 mRNA expression occurs in the CVOs and their neighboring brain regions after the systemic injection of LPS (Laflamme et al., 2001, 2003; Rivest, 2009). We examined whether or not the systemic LPS injection increases the TLR2 protein expression in the CVOs at a dose of 100 μg/kg and whether this LPS pretreatment changes the TLR2-dependent fever and sickness responses. The TLR2 immunoreactivity of the Iba1$^+$ microglia/macrophages in the OVLT, SFO and ME in LPS-injected mice (Fig. 7e-g, e′–g′) was significantly higher than that in control mice (Fig. a–c, a′–c′). However, the LPS-stimulated increase in TLR2 immunoreactivity was not clear in the AP (Fig. 7d, d′, h, h′). Based on these data, the relative fluorescent intensity of TLR2 immunoreactivity was quantified (Fig. 7i). The systemic injection of LPS significantly increased the fluorescence intensity of TLR2 immunoreactivity in both the microglia and macrophages of the OVLT (microglia 9.1 ± 1.3; macrophages 14.2 ± 1.7), SFO (microglia 41.9 ± 2.2; macrophages 34.8 ± 4.5) and ME (microglia 20.9 ± 2.0; macrophages 15.9 ± 1.8), but not in the AP (microglia 11.3 ± 6.0; macrophages 12.9 ± 5.3) in comparison to the control mice (OVLT: microglia 2.9 ± 1.1, macrophages 6.2 ± 0.6; SFO: microglia 7.5 ± 0.9; macrophages 14.9 ± 4.8; ME: microglia 9.2 ± 2.8; macrophages 8.4 ± 1.3; AP: microglia 5.2 ± 0.6; macrophages 13.9 ± 1.6).

Next, we investigated whether or not pretreatment with a systemic injection of LPS changes the Pam3CSK4-induced fever and sickness responses (Figs. 8 and 9). The time schedule of the treatment of LPS and Pam3CSK4 is depicted in Fig. 8a. Mice were pretreated with the intraperitoneal injection of LPS (100 μg/kg) or saline and then kept for 24 h with *ad libitum* access to food and water. Mice received an intraperitoneal injection of Pam3CSK4 or DDW at 24 h after the injection of LPS, and their body temperature, locomotor activity, food and water intake, and body weight were measured. The Pam3CSK4-induced fever in LPS-pretreated mice (LPS + Pam) was significantly higher in comparison to that in the saline-pretreated mice (Saline + Pam) (Fig. 8b). Vehicle DDW caused no significant fever in mice with or without LPS pretreatment.

The systemic injection of Pam3CSK4 significantly increased the fever index in LPS- (LPS-Pam; 15.0 ± 0.9 °Cxh) and saline-pretreated (Saline-Pam; 7.5 ± 1.0) mice in comparison to the saline-DDW control mice (2.3 ± 0.9) (Fig. 9a). However, the fever index of Pam3CSK4-

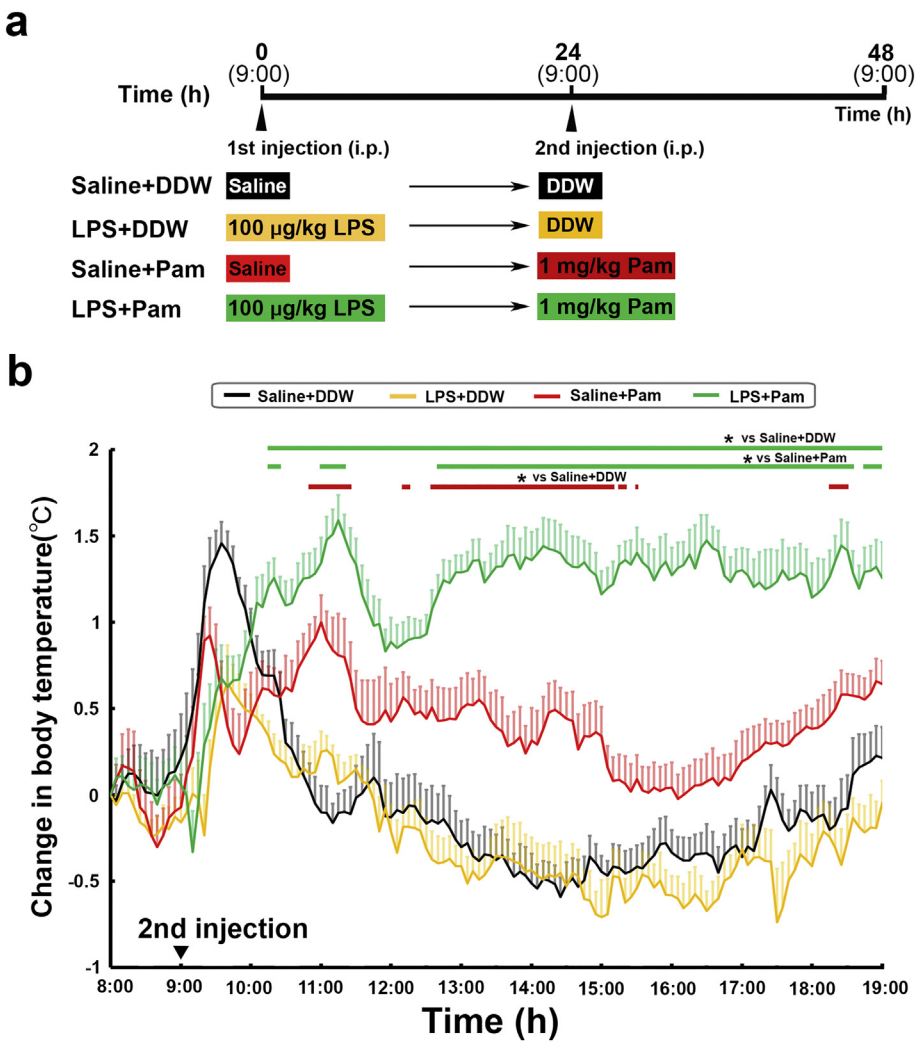

Fig. 8. LPS pretreatment augments the Pam3CSK4-induced fever. a; Schematic representation showing time schedule of first injection of LPS or saline and 2nd injection of Pam3CSK4 or DDW; At 24 h after the intraperitoneal injection of 100 μg/kg LPS, mice received an intraperitoneal injection of either Pam3CSK4 (LPS + Pam) or vehicle DDW (LPS + DDW). At 24 h after the intraperitoneal injection of saline, animals also received the intraperitoneal injection of Pam3CSK4 (1 mg/kg; Saline + Pam) or vehicle DDW (Saline + DDW). b: The abdominal core temperature was measured using a G2 *E*-mitter telemetry system in the ambient temperature at 24 ± 0.5 °C. Mice initially showed stress-induced fever during/after the injection procedure except LPS + Pam group. The intraperitoneal injection of Pam3CSK4 induced significantly more extreme fever in the LPS-pretreated mice (LPS + Pam) in comparison to the saline-treated mice (Saline + Pam). Data (Saline + DDW, $n = 12$; Saline + Pam, $n = 8$; LPS + DDW, n = 8; LPS + Pam, n = 8) are expressed as the mean (± s.e.m.). Green and red lines indicate the period for *P < 0.05, **P < 0.01, ***P < 0.001 among groups (ANOVA with Tukey *post hoc* test). (For interpretation of the references to colour in this figure legend, the reader is referred to the web version of this article.)

stimulated fever in the LPS-pretreated mice (LPS-Pam) was markedly higher than that of the saline-pretreated mice (Saline-Pam). The cumulative locomotor activity in the Pam3CSK4-stimulated animals with (LPS + Pam; 1697.1 ± 248.5) and without (Saline + Pam; 1688.6 ± 146.7) was reduced in comparison to the control mice (Saline + DDW; 3237.6 ± 267.1) (Fig. 9b, Fig. S2). The food (Fig. 9c) and water intake (Fig. 9d) in the Pam3CSK4-stimulated mice with (LPS + Pam) and without (Saline + Pam) LPS pretreatment were also decreased in comparison to the control (Saline + DDW). LPS-treated mice showed a marked reduction in body weight in comparison to saline-treated control mice during the 24 h after the first injection of LPS (Fig. 9e). Pam3CSK4 stimulation significantly reduced the body weight of mice during the 24 h after the second injection of Pam3CSK4, regardless of whether they had received LPS pretreatment (Fig. 9f). The cumulative body weight loss in the Pam3CSK4-stimulated mice with LPS pretreatment was significantly higher than that in those without LPS pretreatment (Fig. 9g). Overall, these data indicate that LPS pretreatment augmented the Pam3CSK4-stimulated fever and body weight loss together with the increased expression of TLR2 in the CVOs.

4. Discussion

TLR2 is the well-known pattern receptor that recognizes a variety of PAMPs from all microbial phyla, including viruses, fungi, bacteria, and parasites and plays crucial roles in the inflammatory and thermogenic response. Until now, however, little has been known about the TLR2-dependent brain pathways that cause inflammatory responses. In the present study, we found that TLR2 was highly expressed in the parenchyma microglia and non-parenchyma macrophages in the CVOs and that the systemic injection of the TLR2 agonist Pam3CSK4 induced NF-κB activation in these two types of brain immune cells. Pam3CSK4 also induced the expression of Fos in the astrocytes of the CVOs and neurons in the inflammation-associated brain regions. Pretreatment with LPS (a TLR4 agonist) augmented the protein expression of TLR2 in the CVOs and the TLR2-dependent fever and sickness responses. These results indicate that the peripheral injection of TLR2 PAMPs stimulates TLR2 on microglia/macrophages in the CVOs and its information relay to the astrocyte-neuronal circuits to regulate inflammatory responses. Moreover, the TLR2-dependent fever and sickness responses are largely augmented by TLR4.

Previously, *in situ* hybridization histochemistry showed the high expression of TLR2 mRNA in the SFO, ME, choroid plexus (Laflamme et al., 2003), and AP (Chakravarty and Herkenham, 2005). Moreover, the TLR2 mRNA-expressing cells in the ME are reported to be positive for microglial/macrophagal marker Iba1 (Laflamme et al., 2001, 2003). In the present study, immunohistochemistry further revealed that TLR2 immunoreactivity in all regions of the CVOs was markedly higher in comparison to other brain regions. Moreover, triple-labeling immunohistochemistry also demonstrated that the TLR2 immunoreactivity was found in both the perivascular macrophages and parenchyma microglia of the CVOs. The perivascular structure of the CVO is largely different from that of the general brain, since a broad perivascular space is present between the endothelial inner basement membrane and the parenchymal outer basement membrane (Miyata,

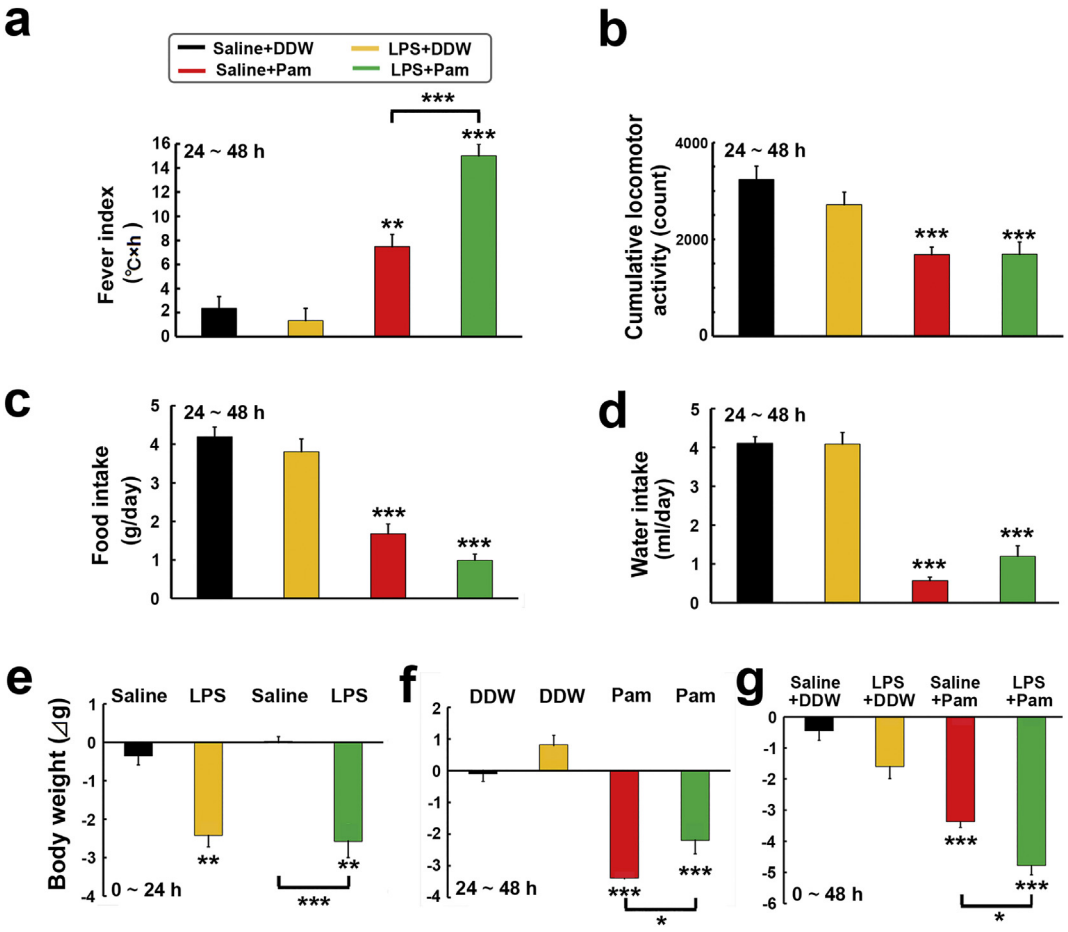

Fig. 9. LPS pretreatment augments the Pam3CSK4-induced fever and sickness responses. a: The fever index was significantly higher in Pam3CSK4-stimulated mice with (LPS + Pam) and without (Saline + Pam) LPS pretreatment compared with the DDW-injected control (Saline + DDW). The fever index of Pam3CSK4-stimulated fever was significantly greater in LPS-pretreated mice (LPS + Pam) than that of the saline-pretreated animals (Saline + Pam). b: The cumulative locomotor activity of the Pam3CSK4-stimulated mice (Saline + Pam, LPS + Pam) was significantly lower than that of the non-stimulated control mice (Saline + DDW). c,d: The food and water intake of the Pam-stimulated mice (Saline + Pam and LPS + Pam) were significantly lower in comparison to the non-stimulated control mice (Saline + DDW). e,f, g: The body weight of mice showed a large decrease during the period from 0 to 24 h after the first injection of LPS (e). The second injection of Pam3CSK4 significantly decreased the body weight of mice with or without LPS pretreatment (f). The cumulative body weight loss of the LPS-pretreated and Pam3CSK4-stimulated (LPS + Pam) mice was significantly greater than that of the saline-pretreated and Pam3CSK4-stimulated mice (Saline + Pam). The period depicted in each panel indicates the time after the first injection of LPS or saline. Data (Saline + DDW, n = 12; Saline + Pam, n = 8; LPS + DDW, n = 8; LPS + Pam, n = 8) are expressed as the mean (± s.e.m.). *P < 0.05, **P < 0.01, ***P < 0.001 among groups (ANOVA with Tukey *post hoc* test).

2015, 2017). Perivascular macrophages are very similar to microglia in their expression of marker proteins, such as Iba1, CD11b, and CX3CR1, and are involved in immune surveillance (Lopez-Atalaya et al., 2018). Thus, we clearly demonstrated that TLR2 is highly expressed in all regions of the CVOs and that its cellular phenotype includes both microglia and macrophages.

In the present study, we found that the intraperitoneal injection of the TLR2 agonist Pam3CSK4 caused NF-κB activation in both the microglia and macrophages of the CVOs. This result was in line with the finding that TLR2 is mainly expressed by the microglia and macrophages. The intraperitoneal injection of macrophage-activating lipopeptide-2 from *Mycoplasma fermentans* induces STAT3 activation in unidentified cells in the CVOs and induces fever (Knorr et al., 2008; Welsch et al., 2012). Since the activation of NF-κB signaling has been shown to be induced in brain endothelial cells by IL-1β (Ching et al., 2007), it cannot be denied that the NF-κB activation of microglia/macrophages is induced by Pam3CSK4-induced IL-1β in the circulation. However, the present study revealed that the systemic injection of Pam3CSK4 did not cause prominent NF-κB activation in the neurons and astrocytes of the CVOs, although IL-1 receptor accessory protein is expressed by the neurons and astrocytes of the SFO (Wei et al., 2015).

High-molecular-weight (HMW) molecules (MW 10,000 to 100,000) cannot reach the parenchyma of the CVOs, but they pass the inner basement membrane to accumulate in the perivascular space of the CVOs (Morita and Miyata, 2012; Miyata, 2015, 2017). The perivascular macrophages in the AP can phagocytize blood-derived HMW molecules in the perivascular space (Morita and Miyata, 2012; Miyata, 2015, 2017). In contrast to HMW molecules, low-molecular-weight (LMW) molecules (MW < 5000) freely pass both the basement membranes to reach the parenchyma (Morita and Miyata, 2012; Miyata, 2015, 2017). TLR2 agonists include a variety of substances; LMW-type agonists such as the lipoteichoic acid (MW 1032) and Pam3CSK4 (MW 1509), and mycoplasma macrophage-activating lipopeptide 2 (MW 2135) and HMW-type agonists such as Zymosan (large variable polysaccharides) and LP44 (MW 44,000). In a previous study, the i.c.v. infusion of Pam3CSK induced significant fever and sickness responses in wild-type mice, but not in TLR2 knockout mice (Jin et al., 2016). The present study showed that the intraperitoneal injection of Pam3CSK caused similar fever and sickness responses to those caused by the i.c.v. infusion of Pam3CSK4. Moreover, the present study showed that NF-κB activation in microglia was prominently significant in the OVLT compared with other CVOs. This result suggests that the OVLT is more

important to sense and transmit the information of peripheral infection of TLR2 pathogens, because the OVLT is intimately associated with generation of fever (Nakamori et al., 1993; Simm et al., 2016). In our previous study, TLR4 was expressed by the astrocytes, and the systemic injection of LPS caused NF-κB activation in the astrocytes of the CVOs (Nakano et al., 2015; Muneoka et al., 2019). LPS has been shown to be detected in parenchyma of the CVOs, suggesting that LPS can pass fenestrated capillaries and reach the parenchymal TLR4 on the astrocytes of the CVOs (Vargas-Caraveo et al., 2017). These results suggest that circulating LMW TLR2 PAMPs can bind directly to TLR2 on microglia/macrophages and that HMW ones can directly stimulate TLR2 on macrophages to activate NF-κB in the CVOs to initiate inflammatory responses. Thus, the CVOs are the brain regions that initiate both the TLR2- and TLR4-dependent inflammatory responses during the early phase of the inflammatory response, whereas their competent cellular phenotype or signaling pathway is different.

The present study showed that the intraperitoneal injection of Pam3CSK4 induced the expression of Fos in the astrocytes of the CVOs. Fos is one of the immediate-early genes, which are powerful tools for identifying activated cells (Chandra and Lobo, 2017). Microglia-astrocyte interactions are required for LPS to induce the the mRNA expression of pro-inflammatory cytokines in the astrocytes, and microglia-derived TNF-α is a critical secondary messenger for the activation of astrocytes (Chen et al., 2012). Astrocytes can respond to inflammatory mediators and cytokines, including IL-1β and TNF-α to upregulate the expression of various cytokines (Carpentier et al., 2005). In our previous studies, STAT3 signaling in astrocytic NSCs has been shown to be important for controlling the inflammatory response of the brain (Yoshida et al., 2016; Muneoka et al., 2019). Moreover, the present study showed that the systemic injection of Pam3CSK significantly elevated the neuronal Fos expression in neighboring hypothalamic regions, such as the MPA, MnPO, ZI, and AH in the hypothalamus. These regions are known to be the main inflammatory brain center driving the sympathetic nerve activity to generate fever (Lazarus et al., 2007; Contreras et al., 2016; Eskilsson et al., 2017). Hypothalamic nuclei such as those in the MPA, MnPO, and AH, have been shown to be the main inflammatory center that drives the sympathetic nerve activity and controls fever production (Lazarus et al., 2007; Contreras et al., 2016; Eskilsson et al., 2017). The electrical stimulation of the actual band in the ZI changes the baseline temperature of brown fat tissue (Kelly and Bielajew, 1996) possibly through the activation of the locus coeruleus, raphe complex, parabrachial area, and medial districts of the pons to the medullary reticular formation (Shammah-Lagnado et al., 1985). A previous study showed that the induction of TLR2 activation by i.c.v. injection of Pam3CSK4 triggered hypothalamic inflammation and the activation of the arcuate nucleus microglia (Jin et al., 2016). Thus, it is possible that brain inflammatory responses are first initiated by TLR2-dependent NF-κB signaling in the macrophages and microglia of the CVOs, and that this information is transmitted to the astrocytes and neurons of the CVOs and neighboring brain regions.

In the present study, we found that LPS pretreatment augmented the expression of TLR2 in the microglia/macrophages of the CVOs. This result was in line with the results of previous studies that showed that LPS pretreatment significantly increased the expression of TLR2 mRNA in the SFO and chloride plexus (Laflamme et al., 2001, 2003; Rivest, 2009). Circulating LPS has limited access to the brain parenchyma due to the BBB, but it can bind to the parenchymal cells in the CVOs (Vargas-Caraveo et al., 2017). In our previous study, TLR4 was shown to be highly expressed in the astrocytes and tanycytes of the CVOs (Nakano et al., 2015; Muneoka et al., 2019). Both intraperitoneal and i.c.v. injections of LPS cause STAT3 activation in the astrocytes and tanycytes of the CVOs (Nakano et al., 2015; Yoshida et al., 2016) and the intraperitoneal injection of LPS induces NF-κB activation (Quan et al., 1997; Chakravarty and Herkenham, 2005; Muneoka et al., 2019) and the expression of Fos (Muneoka et al., 2019) in these glial cells. TLR4 also activates the microglia, which changes their shape from stellate to amoeboid (Lee et al., 2010) and induces a growing and temporal proliferation (Furube et al., 2018). Furthermore, in the present study, the systemic injection of Pam3CSK augmented the fever and sickness responses by LPS pretreatment. Repeated LPS injections over short-term intervals result in attenuated fever, which is called endotoxin tolerance (Beeson, 1947). Animals with acquired tolerance to LPS exhibit less apparent responses to nonlethal LPS doses and survived lethal LPS doses (Freudenberg et al., 1998). In humans, cancer patients with polymicrobial bloodstream infection have higher mortality rates in comparison to those with monomicrobial bloodstream infection (Royo-Cebrecos et al., 2017). Thus, the phenotypes of TLR2- and TLR4-expressing cells are different in the CVOs, but they interact with each other in a coordinated manner and stimulation of both TLRs causes severe fever and inflammatory responses.

Acknowledgements

This work was supported in part by Scientific Research Grants from The Japan Society for the Promotion of Science (16 K07027, 19K06921).

Appendix A. Supplementary data

Supplementary data to this article can be found online at https://doi.org/10.1016/j.jneuroim.2019.576973.

References

Akira, S., Takeda, K., Kaisho, T., 2001. Toll-like receptors: critical proteins linking innate and acquired immunity. Nat. Immunol. 2, 675–680.
Beeson, P.B., 1947. Effect of reticulo-endothelial blockade on immunity to the Shwartzman phenomenon. Proc. Soc. Exp. Biol. Med. 64, 146–149.
Beutler, B., Jiang, Z., Georgel, P., Crozat, K., Croker, B., Rutschmann, S., Du, X., Hoebe, K., 2006. Genetic analysis of host resistance: toll-like receptor signaling and immunity at large. Annu. Rev. Immunol. 24, 353–389.
Botos, I., Segal, D.M., Davies, D.R., 2011. The structural biology of toll-like receptors. Structure 19, 447–459.
Breder, C.D., Hazuka, C., Ghayur, T., Klug, C., Huginin, M., Yasuda, K., Teng, M., Saper, C.B., 1994. Regional induction of tumor necrosis factor alpha expression in the mouse brain after systemic lipopolysaccharide administration. Proc. Natl. Acad. Sci. U. S. A. 91, 11393–11397.
Carpentier, P.A., Begolka, W.S., Olson, J.K., Elhofy, A., Karpus, W.J., Miller, S.D., 2005. Differential activation of astrocytes by innate and adaptive immune stimuli. Glia 49, 360–374.
Chakravarty, S., Herkenham, M., 2005. Toll-like receptor 4 on nonhematopoietic cells sustains CNS inflammation during endotoxemia, independent of systemic cytokines. J. Neurosci. 25, 1788–1796.
Chandra, R., Lobo, M.K., 2017. Beyond neuronal activity markers: select immediate early genes in striatal neuron subtypes functionally mediate psychostimulant addiction. Front. Behav. Neurosci. 11, 112.
Chen, Z., Jalabi, W., Shpargel, K.B., Farabaugh, K.T., Dutta, R., Yin, X., Kidd, G.J., Bergmann, C.C., Stohlman, S.A., Trapp, B.D., 2012. Lipopolysaccharide-induced microglial activation and neuroprotection against experimental brain injury is independent of hematogenous TLR4. J. Neurosci. 32, 11706–11715.
Ching, S., Zhang, H., Belevych, N., He, L., Lai, W., Pu, X.A., Jaeger, L.B., Chen, Q., Quan, N., 2007. Endothelial-specific knockdown of interleukin-1 (IL-1) type 1 receptor differentially alters CNS responses to IL-1 depending on its route of administration. J. Neurosci. 27, 10476–10486.
Contreras, C., Nogueiras, R., Dieguez, C., Medina-Gomez, G., Lopez, M., 2016. Hypothalamus and thermogenesis: heating the BAT, browning the WAT. Mol. Cell. Endocrinol. 438, 107–115.
Eskilsson, A., Matsuwaki, T., Shionoya, K., Mirrasekhian, E., Zajdel, J., Schwaninger, M., Engblom, D., Blomqvist, A., 2017. Immune-induced fever is dependent on local but not generalized prostaglandin E2 synthesis in the brain. J. Neurosci. 37, 5035–5044.
Freudenberg, M.A., Salomao, R., Sing, A., Mitov, I., Galanos, C., 1998. Reconciling the concepts of endotoxin sensitization and tolerance. Prog. Clin. Biol. Res. 397, 261–268.
Furube, E., Morita, M., Miyata, S., 2015. Characterization of neural stem cells and their progeny in the sensory circumventricular organs of adult mouse. Cell Tissue Res. 362, 347–365.
Furube, E., Kawai, S., Inagaki, H., Takagi, S., Miyata, S., 2018. Brain region-dependent heterogeneity and dose-dependent difference in transient microglia population increase during lipopolysaccharide-induced inflammation. Sci. Rep. 8, 2203.
Gay, N.J., Symmons, M.F., Gangloff, M., Bryant, C.E., 2014. Assembly and localization of toll-like receptor signalling complexes. Nat. Rev. Immunol. 14, 546–558.
Hashimoto, M., Tawaratsumida, K., Kariya, H., Kiyohara, A., Suda, Y., Krikae, F., Kirikae, T., Götz, F., 2006. Not lipoteichoic acid but lipoproteins appear to be the dominant

immunobiologically active compounds in Staphylococcus aureus. J. Immunol. 177, 3162–3169.
Imamura, Y., Morita, S., Nakatani, Y., Okada, K., Ueshima, S., Matsuo, O., Miyata, S., 2010. Tissue plasminogen activator and plasminogen are critical for osmotic homeostasis by regulating vasopressin secretion. J. Neurosci. Res. 88, 1995–2006.
Jin, S., Kim, J.G., Park, J.W., Koch, M., Horvath, T.L., Lee, B.J., 2016. Hypothalamic TLR2 triggers sickness behavior via a microglia-neuronal axis. Sci. Rep. 6, 29424.
Kawai, T., Akira, S., 2010. The role of pattern-recognition receptors in innate immunity: update on toll-like receptors. Nat. Immunol. 11, 373–384.
Kelly, L., Bielajew, C., 1996. Short-term stimulation-induced decreases in brown fat temperature. Brain Res. 715, 172–179.
Knorr, C., Hübschle, T., Murgott, J., Mühlradt, P., Gerstberger, R., Roth, J., 2008. Macrophage-activating lipopeptide-2 (MALP-2) induces a localized inflammatory response in rats resulting in activation of brain sites implicated in fever. Brain Res. 1205, 36–46.
Laflamme, N., Rivest, S., 2001. Toll-like receptor 4: the missing link of the cerebral innate immune response triggered by circulating gram-negative bacterial cell wall components. FASEB J. 15, 155–163.
Laflamme, N., Soucy, G., Rivest, S., 2001. Circulating cell wall components derived from gram-negative, not gram-positive, bacteria cause a profound induction of the gene-encoding toll-like receptor 2 in the CNS. J. Neurochem. 79, 648–657.
Laflamme, N., Echchannaoui, H., Landmann, R., Rivest, S., 2003. Cooperation between toll-like receptor 2 and 4 in the brain of mice challenged with cell wall components derived from gram-negative and gram-positive bacteria. Eur. J. Immunol. 33, 1127–1138.
Lazarus, M., Yoshida, K., Coppari, R., Bass, C.E., Mochizuki, T., Lowell, B.B., Saper, C.B., 2007. EP3 prostaglandin receptors in the median preoptic nucleus are critical for fever responses. Nat. Neurosci. 10, 1131–1133.
Lee, S., Zhao, Y.Q., Ribeiro-da-Silva, A., Zhang, J., 2010. Distinctive response of CNS glial cells in oro-facial pain associated with injury, infection and inflammation. Mol. Pain 6, 79.
Lopez-Atalaya, J.P., Askew, K.E., Sierra, A., Gomez-Nicola, D., 2018. Development and maintenance of the brain's immune toolkit: microglia and non-parenchymal brain macrophages. Dev. Neurobiol. 78, 561–579.
Mersmann, J., Berkels, R., Zacharowski, P., Tran, N., Koch, A., Iekushi, K., Dimmeler, S., Granja, T.F., Boehm, O., Claycomb, W.C., Zacharowski, K., 2010. Preconditioning by toll-like receptor 2 agonist Pam3CSK4 reduces CXCL1-dependent leukocyte recruitment in murine myocardial ischemia/reperfusion injury. Crit. Care Med. 38, 903–909.
Miyata, S., 2015. New aspects in fenestrated capillary and tissue dynamics in the sensory circumventricular organs of adult brains. Front. Neurosci. 9, 390.
Miyata, S., 2017. Advances in understanding of structural reorganization in the hypothalamic neurosecretory system. Front. Endocrinol. 8, e275.
Morita, S., Miyata, S., 2012. Different vascular permeability between the sensory and secretory circumventricular organs of adult mouse brain. Cell Tissue Res. 349, 589–603.
Morita, S., Furube, E., Mannari, T., Okuda, H., Tatsumi, K., Wanaka, A., Miyata, S., 2016. Heterogeneous vascular permeability and alternative diffusion barrier in sensory circumventricular organs of adult mouse brain. Cell Tissue Res. 363, 497–511.
Muneoka, S., Murayama, S., Nakano, Y., Miyata, S., 2019. TLR4 in circumventricular neural stem cells is a negative regulator for thermogenic pathways in the mouse brain. J. Neuroimmunol. 331, 58–73.
Nakamori, T., Morimoto, A., Yamaguchi, K., Watanabe, T., Long, N.C., Murakami, N., 1993. Organum vasculosum laminae terminalis (OVLT) is a brain site to produce interleukin-1 beta during fever. Brain Res. 618, 155–159.
Nakano, Y., Furube, E., Morita, S., Wanaka, A., Nakashima, T., Miyata, S., 2015. Astrocytic TLR4 expression and LPS-induced nuclear translocation of STAT3 in the sensory circumventricular organs of adult mouse brain. J. Neuroimmunol. 278, 144–158.
Nguyen, M.T., Gotz, F., 2016. Lipoproteins of gram-positive Bacteria: key players in the immune response and virulence. Microbiol. Mol. Biol. Rev. 80, 891–903.
Oliveira-Nascimento, L., Massari, P., Wetzler, L.M., 2012. The role of TLR2 in infection and immunity. Front. Immunol. 3, 79.
Paxinos, G., Franklin, K.B.J., 2001. The Mouse Brain in Stereotaxic Coordinates: Second Edition. Academic Press, San Diego.
Quan, N., Whiteside, M., Kim, L., Herkenham, M., 1997. Induction of inhibitory factor kappa B alpha mRNA in the central nervous system after peripheral lipopolysaccharide administration: an in situ hybridization histochemistry study in the rat. Proc. Natl. Acad. Sci. U. S. A. 94, 10985–10990.
Rice, L.B., 2006. Antimicrobial resistance in gram-positive bacteria. Am. J. Med. 119, S11–S19.
Rivest, S., 2003. Molecular insights on the cerebral innate immune system. Brain Behav. Immun. 17, 13–19.
Rivest, S., 2009. Regulation of innate immune responses in the brain. Nat. Rev. Immunol. 9, 429–439.
Roth, J., Harré, E.M., Rummel, C., Gerstberger, R., Hübschle, T., 2004. Signaling the brain in systemic inflammation: role of sensory circumventricular organs. Front. Biosci. 9, 290–300.
Royo-Cebrecos, C., Gudiol, C., Ardanuy, C., Pomares, H., Calvo, M., Carratalà, J., 2017. A fresh look at polymicrobial bloodstream infection in cancer patients. PLoS One 12, e0185768.
Rummel, C., Hübschle, T., Gerstberger, R., Roth, J., 2004. Nuclear translocation of the transcription factor STAT3 in the Guinea pig brain during systemic or localized inflammation. J. Physiol. 557, 671–687.
Rummel, C., Voss, T., Matsumura, K., Korte, S., Gerstberger, R., Roth, J., Hübschle, T., 2005. Nuclear STAT3 translocation in Guinea pig and rat brain endothelium during systemic challenge with lipopolysaccharide and interleukin-6. J. Comp. Neurol. 491, 1–14.
Schwandner, R., Dziarski, R., Wesche, H., Rothe, M., Kirschning, C.J., 1999. Peptidoglycan- and lipoteichoic acid-induced cell activation is mediated by toll-like receptor 2. J. Biol. Chem. 274, 17406–17409.
Shammah-Lagnado, S.J., Negrao, N., Ricardo, J.A., 1985. Afferent connections of the zona incerta: a horseradish peroxidase study in the rat. Neuroscience 15, 109–134.
Simm, B., Ott, D., Pollatzek, E., Murgott, J., Gerstberger, R., Rummel, C., Roth, J., 2016. Effects of prostaglandin E2 on cells cultured from the rat organum vasculosum laminae terminalis and median preoptic nucleus. Neuroscience 313, 23–35.
Sisó, S., Jeffrey, M., González, L., 2010. Sensory circumventricular organs in health and disease. Acta Neuropathol. 120, 689–705.
Takeuchi, O., Hoshino, K., Akira, S., 2000. Cutting edge: TLR2-deficient and MyD88-deficient mice are highly susceptible to Staphylococcus aureus infection. J. Immunol. 165, 5392–5396.
Vallieres, L., Rivest, S., 1997. Regulation of the genes encoding interleukin-6, its receptor, and gp130 in the rat brain in response to the immune activator lipopolysaccharide and the proinflammatory cytokine interleukin-1beta. J. Neurochem. 69, 1668–1683.
Vargas-Caraveo, A., Sayd, A., Maus, S.R., Caso, J.R., Madrigal, J.L.M., García-Bueno, B., Leza, J.C., 2017. Lipopolysaccharide enters the rat brain by a lipoprotein-mediated transport mechanism in physiological conditions. Sci. Rep. 7, 13113.
Wei, S.G., Yu, Y., Zhang, Z.H., Felder, R.B., 2015. Proinflammatory cytokines upregulate sympathoexcitatory mechanisms in the subfornical organ of the rat. Hypertension 65, 1126–1133.
Welsch, J., Hübschle, T., Murgott, J., Kirschning, C., Rummel, C., Gerstberger, R., Roth, J., 2012. Fever induction by systemic stimulation with macrophage-activating lipopeptide-2 depends upon TLR2 but not CD36. Innate. Immun. 18, 541–559.
Yoshida, A., Furube, E., Mannari, T., Takayama, Y., Kittaka, H., Tominaga, M., Miyata, S., 2016. TRPV1 is crucial for proinflammatory STAT3 signaling and thermoregulation-associated pathways in the brain during inflammation. Sci. Rep. 6, 26088.
Zahringer, U., Lindner, B., Inamura, S., Heine, H., Alexander, C., 2008. TLR2-promiscuous or specific? A critical re-evaluation of a receptor expressing apparent broad specificity. Immunobiology 213, 205–224.
Zlokovic, B.V., 2011. Neurovascular pathways to neurodegeneration in Alzheimer's disease and other disorders. Nat. Rev. Neurosci. 12, 723–738.